We are IntechOpen, the world's leading publisher of Open Access books Built by scientists, for scientists

6,900
Open access books available

186,000
International authors and editors

200M
Downloads

Our authors are among the

154
Countries delivered to

TOP 1%
most cited scientists

12.2%
Contributors from top 500 universities

WEB OF SCIENCE™

Selection of our books indexed in the Book Citation Index in Web of Science™ Core Collection (BKCI)

Interested in publishing with us?
Contact book.department@intechopen.com

Numbers displayed above are based on latest data collected.
For more information visit www.intechopen.com

Chapter 8

Nanostructured Oxide Semiconductor Compounds with Possible Applications for Gas Sensors

Corneliu Doroftei and Liviu Leontie

Additional information is available at the end of the chapter

http://dx.doi.org/10.5772/intechopen.79079

Abstract

Nanostructured oxide semiconductor compounds have gained a big importance, in basic and mostly in applicative researches, due to their unique properties, and their increased potential of utilization as sensors in various electronic and optoelectronic devices. The development of devices based on semiconductor materials as gas sensors has been visible during the recent years, due to their low manufacturing cost. Because the basic materials and the manufacturing processes are critical for gas sensors high performance, they need to be studied and capitalized in practice. Among the new technologies, the production of nanocrystalline materials and hybrid structures offer huge opportunities to improve sensitivity, selectivity and response time, as a consequence of the intensification of gas-sensor interaction. In this study, a series of nanostructured oxide semiconductor compounds with a spinel-type structure and perovskite, respectively, based on transition metals and synthesized by the sol-gel self-combustion method, with possible applications for resistive gas sensors, are presented.

Keywords: nanostructured materials, oxide semiconductors, sol-gel self-combustion, structural properties, gas-sensing properties

1. Introduction

In order to improve the environmental conditions, in certain spaces, monitoring and control systems are needed. These must be able to quickly and safely detect the gas-polluting sources and to compare their emissions with the accepted standards. Until now, the air pollution measurements were performed with analytical instruments using optical spectroscopy or mass chromatograph spectrometry for gases.

IntechOpen

© 2018 The Author(s). Licensee IntechOpen. This chapter is distributed under the terms of the Creative Commons Attribution License (http://creativecommons.org/licenses/by/3.0), which permits unrestricted use, distribution, and reproduction in any medium, provided the original work is properly cited. CC BY

The optical systems measure the absorption spectrum after the target gas was excited by light. Such a sensor needs a complex system: a monochromatic excitation source and an optical sensor to analyze the absorption spectrum [1].

The spectroscopic systems are based on the direct analysis of the molecular mass or of the vibration spectrum of the target gas. Such a sensor can measure quantitatively, with a very good precision, the composition of various gases. The mass spectrometer and the gas chromatograph are the most important systems of spectroscopic gas sensors; yet, at the same time, they are very expensive, hard to implement in reduced spaces, and can rarely be used in real time [1].

Instead, a compact, robust, highly performing and low-cost gas sensor can be a very attractive alternative to the classical devices used for environment monitoring. A series of recent researches [2–7] have been focused for the development of solid gas sensors having as sensitive element oxide semiconductor materials, among which are the spinels and perovskites, and their performances began to be improved.

The main characteristics of the sensors are field of application, sensitivity, selectivity, resolution (the smallest measurable increment of the stimulus), promptitude (rate of reaction to stimuli variation), accuracy (measuring error in percentages reported to the entire scale), sensor size and mass, operating temperature and environmental conditions, life time (in hours or in operating cycles), long-term stability, and cost.

Sensitivity is the device characteristic perceived as the variation of physical and chemical properties of the material exposed to gas.

Selectivity represents the characteristic through which a sensor element can detect a certain target gas from a gas mix.

Stability represents the characteristic through a sensor that is able to give the same results, under the same experimental conditions, after the longest operating time possible.

Nowadays, there is a clear tendency to search for new types of spinel or perovskite nanostrutures and to use new synthesis techniques for the preparation of novel sensor materials in massive form (bulk), thick layers or thin layers. The use of a large number of dopants is meant to increase the sensitivity and selectivity of spinel or perovskite gas sensors. Efforts are made to extend the range of operating temperatures and to lower the optimal operating temperature, and to reduce the power consumption of the sensing element. The resistive sensors made of thin layers present the advantage that has small power consumption; yet, they are sensitive to physical and chemical contamination and are rarely regenerable [1].

The systematic studies on a large number of oxide compounds have proved that the variation of the electric conductivity in the presence of some gases in the air constitutes a common phenomenon for the oxide compounds, including spinels and perovskites [8]. The sign of the response, that is, the increase or decrease of the electric resistivity, is determined by the semiconductor type, *p* or *n*, as well as by the oxidizing or reducing character of the gas. The sensitivity of an oxide semiconductor sensor can be generally improved by doping, thus modifying the charge carrier concentration and mobility, or by microstructural modifications, for example, by reducing the particle dimensions to the nanosized range.

http://dx.doi.org/10.5772/intechopen.79079

The modification of the electric conductivity of the sensing material exposed to the specific gas is mainly the result of the reactions that occur at the sensor surface through the modification of the adsorbed oxygen concentration [9–11]. The oxygen-adsorbed ions at the material surface extract the electrons from the material and create a potential barrier, which restricts the electron movement and conductivity. When the reacting gases combine with this oxygen, the height of the potential barrier is diminished and the gas conductivity increases accordingly. This conductivity change is directly related with the amount of the specific gas present in the environment, whence the possibility to determine the gas presence and concentration [12–14]. These gas sensor reactions appear at diverse temperatures, generally between 100 and 600°C, and the sensor needs to be positioned at the temperature of the maximum response.

One of the main challenges for the developers of spinel-type or perovskite gas sensors is to increase their selectivity. Currently, there are two general approaches for enhancing the selective properties of sensors. The first aims at preparing a material, which is specifically sensitive to a certain gas and has a reduced or zero cross-sensitivity to other compounds that may be present in the working atmosphere. With this purpose, the optimal temperature, the nature of doping elements, and their concentrations are investigated. Nonetheless, it is usually very difficult to achieve an absolutely selective oxide gas sensor in practice. Practically, most of the materials possess cross-sensitivity at least to humidity and other vapors or gases. Another approach is based on the preparation of materials able to discriminate between several gases in a mixture. It is impossible to do this by using a single signal from the sensor. This discrimination can be usually reached either by modulating the sensor temperature [15–20] or by using a sensor array [21–23]. In the former case, such discrimination is possible because of the different optimum operating temperatures for different gases. In the latter case, N signals are obtained simultaneously from N sensors, which usually differ from each other through the doping element, doping ratio, grain size, and/or temperature.

The sensor selectivity is influenced by several factors, such as the surface energy band diagram, energy of gas molecule, and the amount of gas adsorbed on the sensing material at different operating temperatures [24]. Therefore, further investigations will be necessary in order to clarify the mechanism of selectivity.

2. Reports from the specialized literature on a series of oxide semiconductor compounds used for resistive gas sensors

The specialized literature of the recent years reports a series of spinels and perovskites used to obtain gas sensors [25–39].

The spinel-type oxide semiconductors with a general formula of AB_2O_4 have demonstrated to be good materials for the detection of both oxidizing and reducing gases [25–33]. Kapse [35] conducted a study on the sensitivity of spinelic oxide compounds ($NiFe_2O_4$, $ZnFe_2O_4$, $MgFe_2O_4$, $ZnAl_2O_4$, $CoAl_2O_4$ and $MgAl_2O_4$) synthesized by citrated sol–gel technique for various gases (H_2S, NH_3, C_2H_5OH, LPG). The author obtains the best values of the magnesium spinel sensitivity ($MgFe_2O_4$) for H_2S (4.8), C_2H_5OH (12.4), LPG (6.3) at an operating temperature of 325°C

and within the $CoAl_2O_4$ spinel for NH_3 (1.3) at an operating temperature of 150°C and a concentration of 50 ppm. Sutkaa et al. [36] investigated the nickel ferrite with zinc substitutes ($Ni_{1-x}Zn_xFe_2O_4$), p-type semiconductors with increased porosity, predominantly open pores. The samples were synthesized by the sol–gel self-combustion method. For the $NiFe_2O_4$ sample, for a concentration of 500 ppm acetone vapors in the air, they obtain a sensitivity *S* of 3.7 at an optimal operating temperature of 275°C.

Regarding a series of perovskites of type ABO_3, Wang et al. [37] reported the utilization of the nanocrystalline $BaMnO_3$ perovskite having an *n*-type semiconductor behavior as a sensor selective to O_2, with low operating temperatures. Hara et al. [38] have reported a study on perovskites from the $SrTiO_3$ family as O_2 selective sensors, working at the room temperature. The undoped material exhibits high sensitivity, but its resistivity is extremely high, which makes it unusable in practice. It has been found that by Nb^{5+} doping, the sensor resistivity decreases, but its sensitivity also decreases. The same happens for Fe^{3+} doping. By doping with Cr^{3+}, a high decrease of resistivity was obtained, while the sensitivity remains the same. Gaudhari et al. [39] carried out a study on the Ba-doped nanostructured perovskite $SmCoO_3$ as selective sensor for CO_2, working at a temperature of 425°C. For an Sm substitution with Ba ($Sm_{0.9}Ba_{0.1}CoO_3$), a decrease in the optimum operating temperature from 425 to 370°C and a diminution of the response time are obtained.

3. Obtaining nanomaterials by the sol-gel self-combustion method

The classical method for oxide semiconductor preparation implies oxides milling, homogenization, and sintering. Since the size of the milled particles is quite big, and their homogenization is not perfect, a longer sintering operation is necessary to obtain a material with a unitary composition. During sintering, the crystallites increase up to dimensions of the order of micrometer. In order to avoid the crystallite increase phenomenon, the reaction duration must be reduced, and the compounds entering the reaction need to be homogenized at a molecular scale.

The method presented here, named sol-gel self-combustion [40–45], accomplishes the homogenization at the molecular level by introducing compounds in the form of nitrates solutions in a colloidal medium (**Figure 1**). With a view to limit the dimensions of hydroxide particles to a nanometer level and to avoid the flocculation phenomenon, the co-precipitation reaction does not occur in a simple aqueous solution, but in a colloidal solution. The colloid molecules surround the hydroxide microcrystals just after their formation and hinder their rapid growth, thus avoiding their agglomeration. The hydroxide particles remain in the place of their generation, thus providing the homogenization of hydroxide mixture. In order to be certain of the final material composition, one uses reagents, such that after the reaction of hydroxides co-precipitation, the operations of settlement, washing or filtering are no longer necessary, because the secondary reaction products are volatile or eliminable as gases or vapors through subsequent reactions.

Through an exothermic reaction in the form of a quick combustion, one obtains the semiconductor material in the form of an ultra-fine homogeneous powder. In order to obtain very small-size (nanometric) particles of oxide semiconductor material, the reactions of hydroxides calcinations and the formation of oxide compounds occur at a very short time interval (of the

http://dx.doi.org/10.5772/intechopen.79079

order of microseconds) under the form of an autonomous combustion. The substances necessary for combustion result from the reaction of hydroxides formation itself, if adequate reagents are used in the precipitation reaction.

Because the reaction lasts a few seconds, the crystals do not have enough time to grow. The final dimension of the particle of oxide semiconductor material, as well as its structure and properties, is obtained after a heat treatment, during which the process of material crystallization and crystallites growth up to the necessary size occurs. The treatment temperature and duration are, in all the cases, smaller than those necessary for sintering according to classical methods, due to the high homogeneity of the mix.

This method provides a good product homogenization. At the same time, due to the absence of settling, filtering, or washing operations, one has the certitude of material composition.

The sol-gel self-combustion method permits to obtain an ultra-fine, homogeneous powder, with particles of nanometric size, within a narrow dimension range, and a pronounced porosity (as

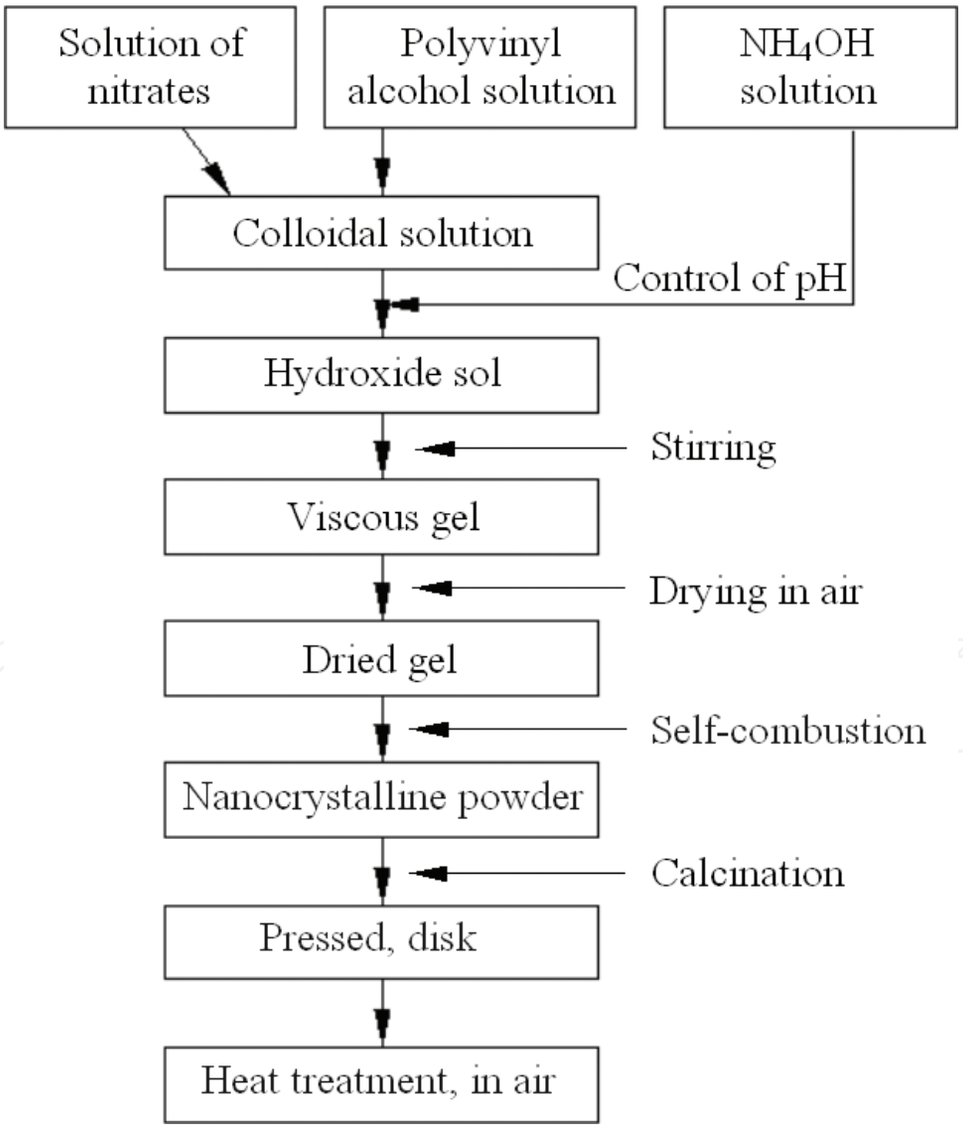

Figure 1. Stages of obtaining materials by sol-gel self-combustion method.

the open pores prevail), which favors gas access inside the samples. This open-pores system appeared during the self-combustion reaction, through which a large amount of gases was eliminated. This porous structure appears at all the oxidic compounds prepared through this method [45–49].

4. Nanostructured spinels and perovskites used for resistive gas sensors

In this subsection, a series of the spinels ($Mg_{1-x}Sn_xFe_2O_4$ where x = 0, 0.1) and perovskites ($La_{0.8}Pb_{0.2}Fe_{1-x}Zn_xO_3$ where x = 0, 0.05, 0.1, 0.2) obtained by the sol-gel self-combustion method used to achieve resistive gas sensors are presented and characterized.

4.1. Gas sensors: obtaining and characterization

Nanograined spinelic and perovskite powders of nominal compositions: $MgFe_2O_4$ (MFO-0), $Mg_{0.9}Sn_{0.1}Fe_2O_4$ (MFO-1) and $La_{0.8}Pb_{0.2}FeO_3$ (LPFO-0), $La_{0.8}Pb_{0.2}Fe_{0.95}Zn_{0.05}O_3$ (LPFO-1), $La_{0.8}Pb_{0.2}Fe_{0.9}Zn_{0.1}O_3$ (LPFO-2), $La_{0.8}Pb_{0.2}Fe_{0.8}Zn_{0.2}O_3$ (LPFO-3), respectively, were prepared by the sol-gel self-combustion method using polyvinyl alcohol (PVA) as fuel and as colloidal medium [50, 51]. The method included the following procedures: dissolution of metal nitrates (stoichiometric amounts of analytical grade) 10% metal in deionized water, the addition of polyvinyl alcohol solution (10% in deionized water, metal/PVA ratio is 1/1), the addition of ammonia to increase pH to about 8, stirring at 80°C, drying the gel at 100–120°C, and finally self-combustion. The combusted powders were calcined at 500°C for 30 min to eliminate any residual carbon and organic compounds [50, 51].

The reactions for the basic compositions (x = 0) can be schematized as follows [30, 51]:

$$2 \cdot Fe(NO_3)_3 + Mg(NO_3)_2 + 8 \cdot NH_4OH \rightarrow 2 \cdot Fe(OH)_3 + Mg(OH)_2 + 8 \cdot NH_4NO_3 \quad (1)$$

$$2 \cdot Fe(OH)_3 + Mg(OH)_2 \rightarrow Fe_2O_3 + MgO + 4 \cdot H_2O \quad (2)$$

$$Fe_2O_3 + MgO \rightarrow MgFe_2O_4 \quad (3)$$

and

$$La(NO_3)_3 + 3 \cdot NH_4OH \rightarrow La(OH)_3 + 3 \cdot NH_4NO_3 \quad (4)$$

$$Pb(NO_3)_2 + 2 \cdot NH_4OH \rightarrow Pb(OH)_2 + 2 \cdot NH_4NO_3 \quad (5)$$

$$Fe(NO_3)_3 + 3 \cdot NH_4OH \rightarrow Fe(OH)_3 + 3 \cdot NH_4NO_3 \quad (6)$$

$$C_2H_3OH + 5 \cdot NH_4NO_3 \rightarrow 2 \cdot CO_2\uparrow + 12 \cdot H_2O\uparrow + 8 \cdot N_2\uparrow + Q \quad (7)$$

$$2 \cdot La(OH)_3 + Pb(OH)_2 + 2 \cdot Fe(OH)_3 \rightarrow La_2O_3 + PbO + Fe_2O_3 + 7 \cdot H_2O\uparrow \quad (8)$$

$$0.8 \cdot La_2O_3 + 0.4 \cdot PbO + Fe_2O_3 + 0.1 \cdot O_2 \rightarrow 2 \cdot La_{0.8}Pb_{0.2}FeO_3 \quad (9)$$

http://dx.doi.org/10.5772/intechopen.79079

The resulting powders were subjected to cold pressing in disk-shaped samples (17-mm diameter, 1.2-mm thick), followed by heat treatment in air for 1100°C/240 min (spinels) and 900°C/40 min (perovskites) [33, 47, 50, 51].

The structure and surface properties of the heat-treated samples were investigated by X-ray diffraction (XRD), scanning electron microscopy (SEM), and energy-dispersive X-ray analysis (EDX).

For electrical measurements, a heat-treated disk was silvered on both flat surfaces. The sensor element was executed by deposing two comb-type silver electrodes on one face of the heat-treated disk using the "screen-printing" method. For the gas-sensing measurements, the sensor element was mounted on a heater capable of controlling the operating temperature and placed in a glass chamber provided with a gas homogenizer and connected to a gas-volumetric dosing device. The gas-sensing properties were investigated at various operating temperatures, included in the range of 100–420°C. The test gases used were ethanol (C_2H_5OH) and acetone (C_3H_6O) at various concentrations. The sensitivity (sensing response), S, for sensor elements made with spinel-type materials, was defined as the ratio [31, 33, 36, 50]

$$S = \frac{\Delta R}{R_a} = \frac{|R_a - R_g|}{R_a} \tag{10}$$

and for sensor elements made with perovskite-type materials, it was defined as the ratio [51–53]

$$S = \frac{R_g}{R_a} \tag{11}$$

where R_a and R_g are the sensor resistance in air and in the presence of the test gas, respectively.

4.2. Results and discussion

4.2.1. Structural properties

From the X-ray diffractometry performed for the samples presented, it was found that the MFO samples present a cubic structure of spinel type, while the LPFO samples present an orthorhombic structure perovskite type, as a result, the heat treatments in air, specific for each sample (**Table 1**). The samples have a good crystallinity in the specified thermal treatment conditions. The structural characteristics of the samples obtained from X-ray diffractometry (XRD) and from analyses by a scanning electron microscope (SEM) [33, 50] are shown in **Table 1**.

Generally, the samples are characterized by a very fine structure being composed of aggregates of nanograins with irregular shapes and sizes, with a pronounced porosity and channels that are favoring the adsorption or desorption of the gas. **Figure 2(a–d)** shows the SEM micrographs for the MFO-0, MFO-1, LPFO-0, and LPFO-2 samples where it is possible to highlight the extremely fine structure of the granule samples having a mean size of about 100 nm for the MFO-1 sample and of about 200 nm for the LPFO-2 sample. The studied samples are characterized by a high porosity (45–65%) and a specific surface area in the domain of 5–24 m^2/g. The gas sensitivity depends largely on the microstructure.

Sample symbol	Lattice constants (Å)	Average particle size D_m (nm)	Bulk density d (g/cm^3)	Porosity p (%)	Specific surface area A_{sp} (m^2/g)
MFO-0	a = 0.8354	500	2.40	45.8	5.0
MFO-1	a = 0.8352	100	2.52	51.6	23.8
LPFO-0	a = 5.5675 b = 7.8648 c = 5.5563	250	3.60	48.56	6.66
LPFO-1	a = 5.5679 b = 7.8665 c = 5.5571	230	3.40	51.49	7.67
LPFO-2	a = 5.5685 b = 7.8673 c = 5.5577	200	3.06	56.41	9.80
LPFO-3	a = 5.5688 b = 7.8685 c = 5.5584	150	2.50	64.50	16

Table 1. Structure characteristics of investigated samples.

The chemical elemental composition of the studied samples was confirmed by the energy-dispersive X-ray spectra (EDX). The obtained chemical elemental composition is typical for these compounds (any foreign element is absent). **Figure 2(e)** presents the EDX spectrum for the LPFO-2 sample.

4.2.2. Gas-sensing properties

The samples show n-type (MFO) and p-type (LPFO) semiconductor characteristics within the studied temperature range. Electrical resistivity measurements in air (ρ_a) at room temperature indicated very high values, over 10^6 Ω·cm. Thermal activation energy is about 0.4 eV for the MFO-0 sample and about 0.6 eV for the other studied samples.

In regard to gas-sensing properties, the sensitivity of the electric resistance to ethanol and acetone vapors in air was investigated. **Figures 3** and **4** show the sensitivity characteristics for the MFO (spinel-type) samples according to the operating temperatures, while these samples were exposed to saturated ethanol or acetone vapors, and **Figures 5** and **6** show the sensitivity characteristics for the LPFO (perovskite-type) samples according to the operating temperatures, while exposed to a concentration of 400 ppm ethanol or acetone vapors.

The gas sensitivity is strongly related to the working temperature, material composition, mean particle size, and porosity [50]. In the studied operating temperature range, the sensitivities increase with the increase of the temperature reaching maximum values (at temperatures called optimal operating temperatures) and then the sensitivities decrease slightly [54–56].

For MFO samples (**Figures 3** and **4**), the gas sensitivity increased with the increasing operating temperature and reached a maximum value at an optimum operating temperature (T_{op}) of

http://dx.doi.org/10.5772/intechopen.79079

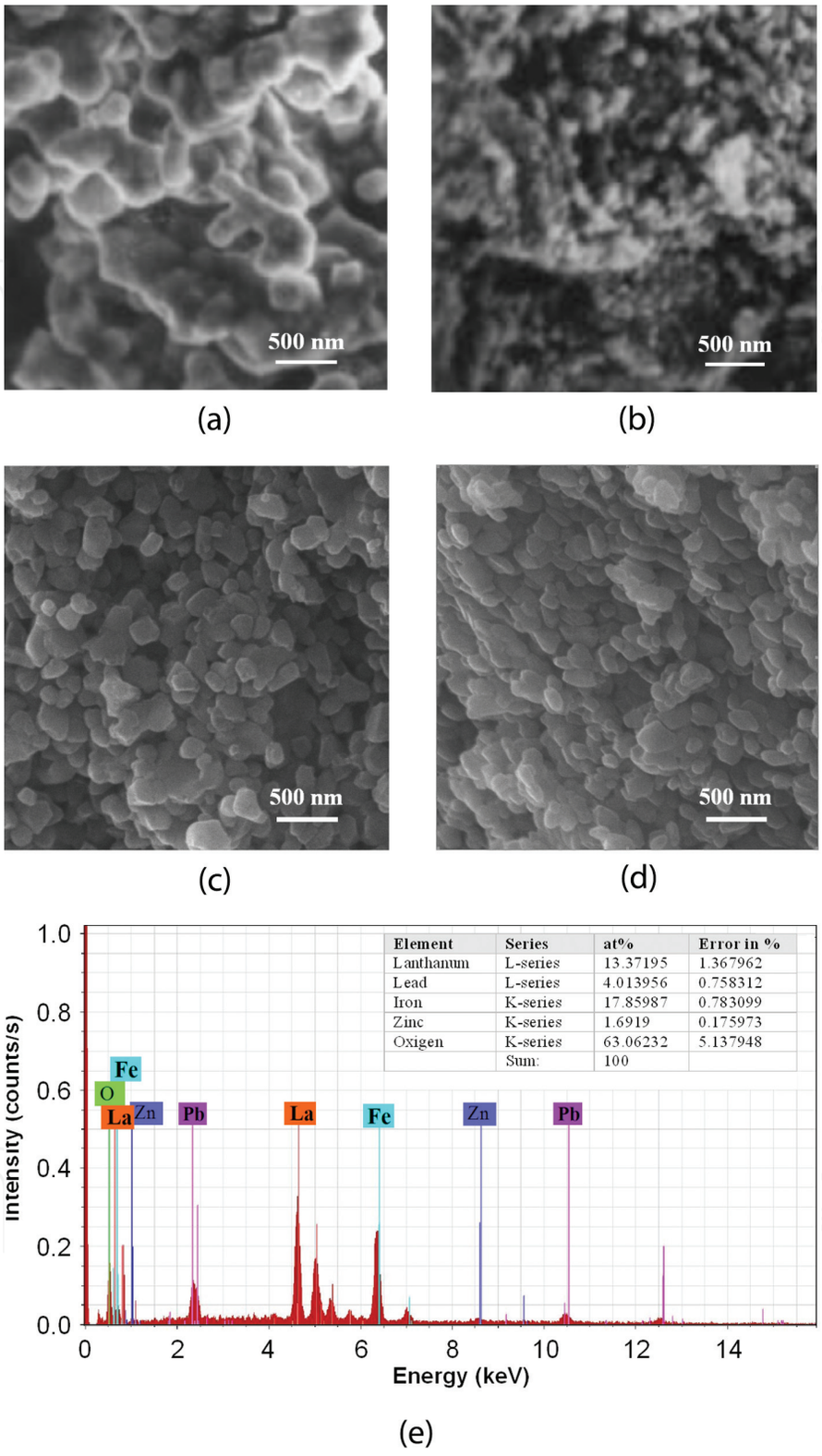

Figure 2. SEM micrographs for the MFO-0 (a), MFO-1 (b), LPFO-0 (c), and LPFO-2 (d) samples and EDX spectra (e) for the LPFO-2 sample [47, 50, 51].

about 380°C. The sensitivity to acetone vapors (**Figure 4**) is higher than that to ethanol vapors (**Figure 3**) for both samples (MFO-0 and MFO-1). The best sensitivity, 0.82, was obtained for the sample that has tin substitutions (MFO-1) to acetone vapors at an optimum operating

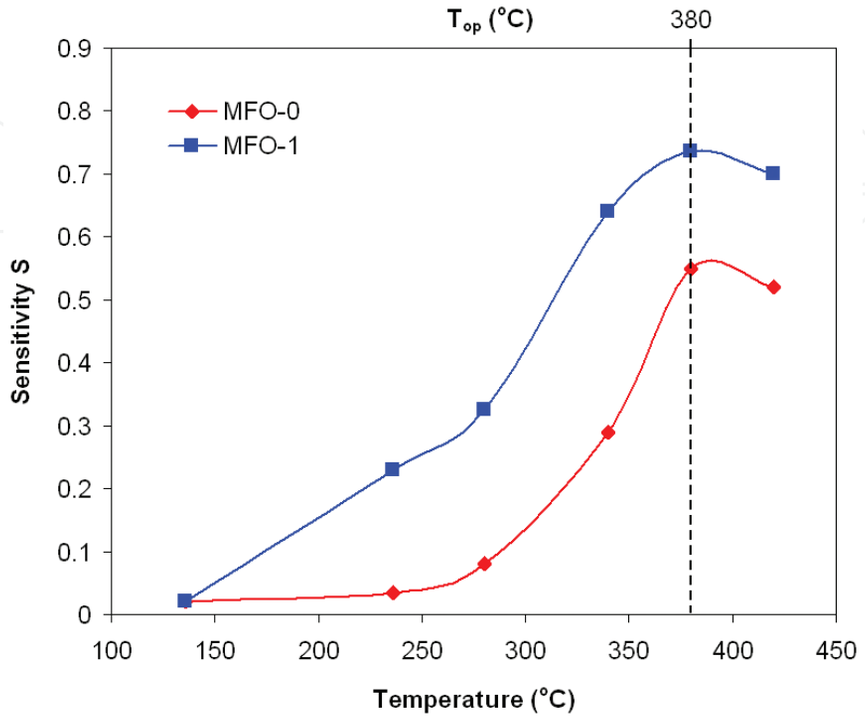

Figure 3. Sensitivity versus operating temperature characteristics for studied spinels at ethanol vapors [50].

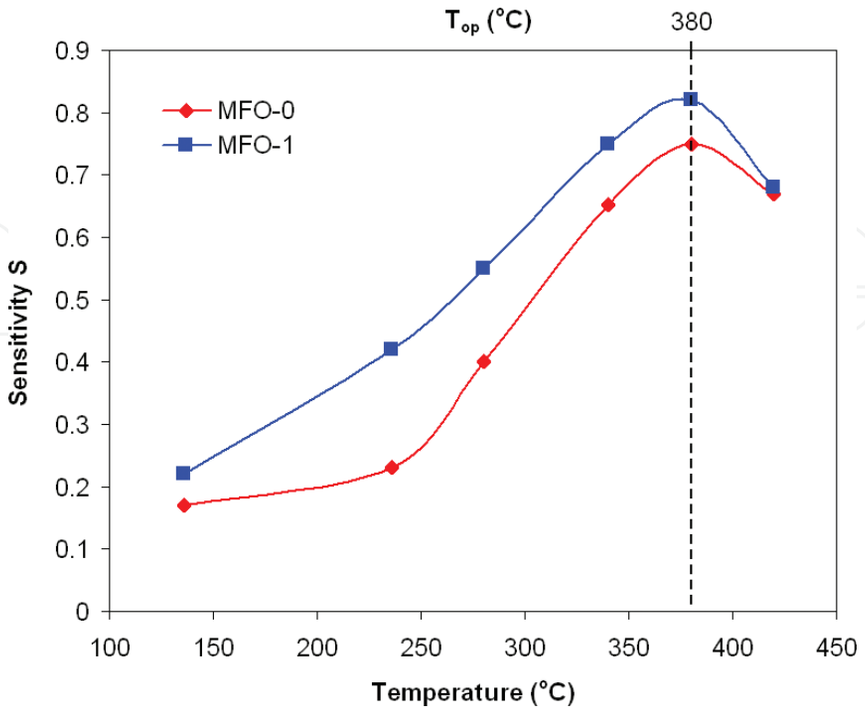

Figure 4. Sensitivity versus operating temperature characteristics for studied spinels at acetone vapors [50].

http://dx.doi.org/10.5772/intechopen.79079

temperature of 380°C. The obtained results correlate well with the grain size changes from 500 to 100 nm (**Table 1**). The sensitivity has been improved by reducing the grain size. Martins et al. [50, 57] analyzed the effect of particle size on the sensitivity of ZnO film and reported a

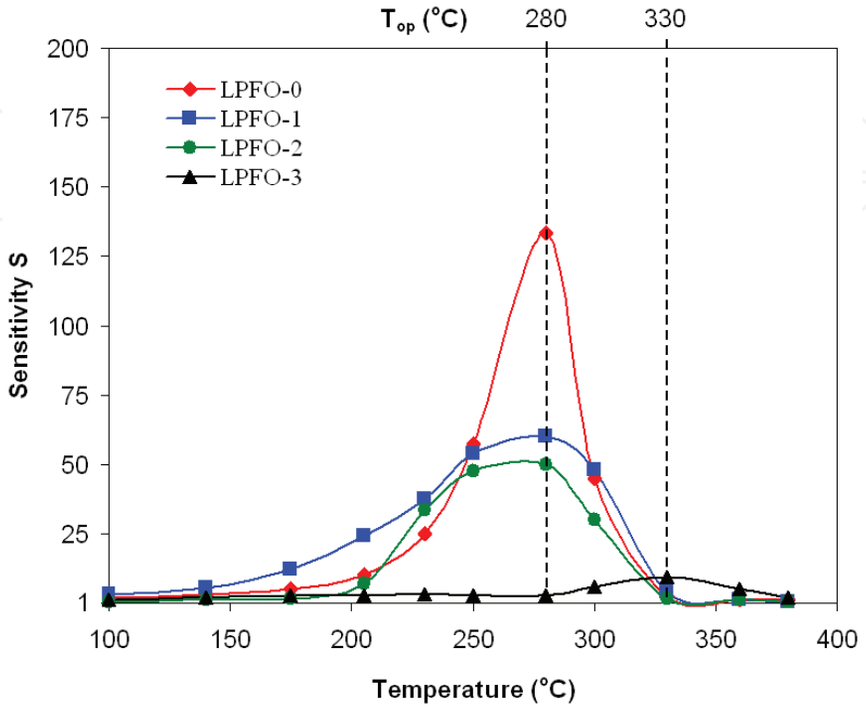

Figure 5. Sensitivity versus operating temperature characteristics for studied perovskites at ethanol vapors [51, 53].

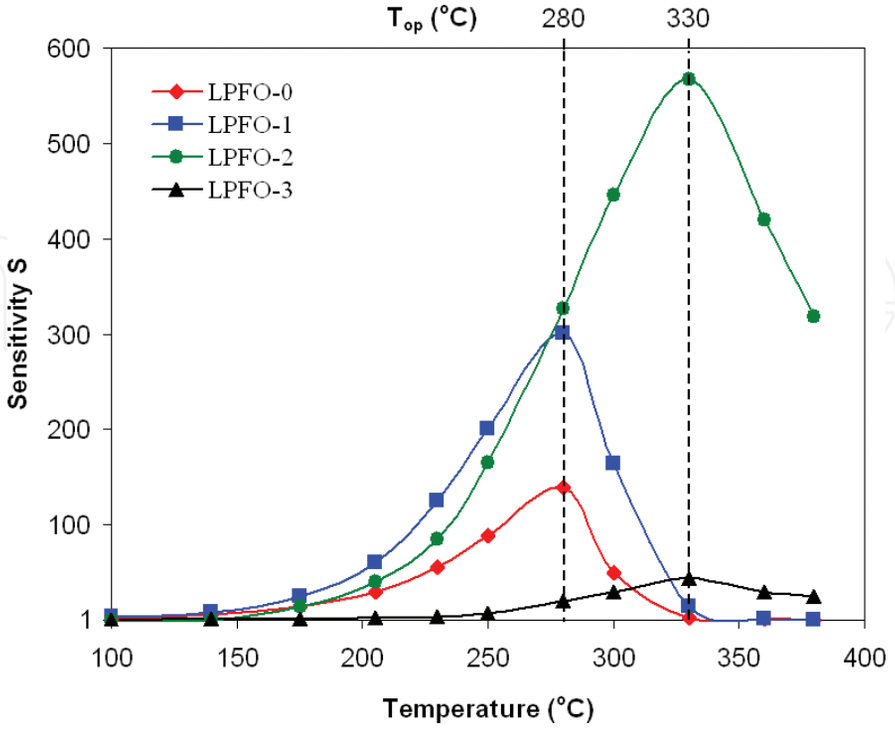

Figure 6. Sensitivity versus operating temperature characteristics for studied perovskites at acetone vapors [51, 53].

significant increase of the sensitivity as the grain size decreases from 120 to 4 nm. Also, the porous structure promotes the increase of the sensitivity. If the sensor material is porous, the gas will easily penetrate into the internal part of the sintered material, resulting in a large change in the resistance (i.e., a large sensitivity). This may be referred to as a structure effect. These results suggest that the role of tin in $MgFe_2O_4$ sample is to facilitate the oxidation of reducing gases [50].

Due to the oxidizing reaction, in the oxide semiconductors, the oxygen vacancies (point defects) appear, which change the electrical conductivity (the free electron concentration increases for the samples with n-type semiconductor behavior, analog the gaps concentration increases for the samples with p-type semiconductor behavior).

For LPFO samples, the sensitivity of ethanol (**Figure 5**) decreases with increasing Zn^{2+} ion concentration from 133 for LPFO-0 sample to 10 for LPFO-3 sample. The sensitivity of LPFO-1 and LPFO-2 samples is somewhere between and close to 50 for both samples. The optimum operating temperature remains around 280°C at the samples with x = 0, 0.05 and 0.1, and increases to 330°C for x = 0.2. The effect of Fe^{3+} ions substitution by Zn^{2+} ions consists in the diminution of the sensitivity to ethanol [51].

The sensitivity to acetone (**Figure 6**) increases very much with the increase of the Zn^{2+} ions concentration from 140 at the sample with x = 0–560 at the sample with x = 0.1. For the concentration x = 0.2, the sensitivity suddenly decreases to 45, as in the case of ethanol. The optimum operating temperature is of 280°C for the samples with x = 0 and 0.05 and increases at 330°C for x = 0.1 and 0.2. The effect of the concentration *x* of Zn^{2+} ions is a spectacular increase of the sensitivity up to x = 0.1, after which the sensitivity strongly decreases for higher concentrations [51].

When the C_2H_5OH (ethanol) or C_3H_6O (acetone) gas is introduced, a chemical reaction occurs between C_2H_5OH and C_3H_6O, respectively, and the adsorbed oxygen [51, 53]:

$$C_2H_5OH_{gas} + 6 \cdot O^{n-}(ads) \rightarrow 2 \cdot CO_{2ads} + 3 \cdot H_2O_{ads} + 6 \cdot ne \quad (12)$$

$$C_3H_6O + 8 \cdot O^{n-}(ads) \rightarrow 3 \cdot CO_{2ads} + 3 \cdot H_2O_{ads} + 8 \cdot ne \quad (13)$$

Electrons released from the reaction would annihilate the holes. Hence, the material resistivity increased. As each acetone molecule produces 8n electrons, that is, the highest number among the two gases, and the molar concentration was the same for the studied gases, the increase of the sensing element resistivity in the presence of acetone is the highest [51]. This suggests that $La_{0.8}Pb_{0.2}Fe_{1-x}Zn_xO_3$ sensors are applicable to detect these gases, especially acetone vapors. The substitution of Fe^{3+} ions by Zn^{2+} ions in $La_{0.8}Pb_{0.2}FeO_3$ intervenes directly, but in a different manner in the sensing mechanism of these gases. For ethanol, the sensitivity decreases with an increasing concentration of Zn^{2+} (x) ions, while for acetone, the sensitivity increases with the increase of *x* value, but decreases for x > 0.1. Therefore, in order to clarify the mechanism of sensitivity, especially to acetone, further investigations will be necessary [51].

http://dx.doi.org/10.5772/intechopen.79079

5. Conclusions

Nanostructured oxide semiconductor compounds have gained a big importance, in basic and mostly in applicative researches, due to their unique properties, their increased potential of utilization as sensors in various electronic and optoelectronic devices. The development of devices based on semiconductor materials as gas sensors has been visible during the recent years, due to their low manufacturing cost.

The mass spectrometer and the gas chromatograph are the most important systems of spectroscopic gas sensors; yet, at the same time, they are very expensive, hard to implement in reduced spaces and can rarely be used in real time.

Instead, a compact, robust, highly performing, and low-cost gas sensor can be a very attractive alternative to the classical devices used for environment monitoring. A series of recent researches have focused on the development of solid gas sensors having as sensitive element oxide semiconductor materials, among which are the spinels and perovskites, and their performances began to be improved.

In this chapter, the structural, morphological, and sensory characteristics of some porous oxide semiconductor compounds with a spinel-type structure ($Mg_{1-x}Sn_xFe_2O_4$; x = 0, 0.1) or with a perovskite-type structure ($La_{0.8}Pb_{0.2}Fe_{1-x}Zn_xO_3$; x = 0, 0.05, 0.1, 0.2) were presented.

These compounds were prepared by the sol-gel self-combustion method. After the thermal treatments in air, the samples attain corresponding crystalline structure (spinel-type or perovskite-type, respectively).

The spinel-type samples are characterized by a very fine structure (100–500 nm) with an accentuated porosity (46–65%) and channels that favor the adsorption or desorption of the gas around particle agglomerates. Samples show a semiconductor behavior with a thermal activation energy between 0.4 and 0.6 eV. The gas sensitivity is strongly related to the working temperature, material composition, mean particle size, and porosity.

In the case of these samples, the gas sensitivity increased with the increasing operating temperature and reached a maximum value at an optimum operating temperature (T_{op}) of about 380°C. The sensitivity to acetone vapors is higher than that to ethanol vapors for both samples (x = 0 and x = 0.1). The best sensitivity, 0.82, was obtained for the sample that has tin substitutions (x = 0.1) to acetone vapors at an optimum operating temperature of 380°C. The obtained results correlate well with the grain size changes from 500 to 100 nm.

The perovskite-type compounds exhibit orthorhombic symmetry (space group Pnma) and crystallizes in the perovskite-like cell of $LaFeO_3$, having a porous granular and a uniform structure. The average grain size decreases from 250 to 150 nm with the increase of Zn concentration. The porosity of the samples increases with increasing Zn concentration from 31.11 to 46.78%. The sensor elements show p-type-semiconducting properties for all studied gases within the temperature range of 100–380°C. Through the substitution of the Fe^{3+} ions by Zn^{2+} ions (x = 0.1), the sensor element has the best response to acetone. At a concentration of 400 ppm gas at the operating temperature of 330°C, the response to acetone is spectacular (560).

Conflict of interest

The authors declare that there are no conflicts of interest.

Author details

Corneliu Doroftei[1]* and Liviu Leontie[1,2]

*Address all correspondence to: docorneliug@gmail.com

1 Integrated Center for Studies in Environmental Science for North-East Region, Alexandru Ioan Cuza University of Iasi, Iasi, Romania

2 Faculty of Physics, Alexandru Ioan Cuza University of Iasi, Iasi, Romania

References

[1] Doroftei C, Iacomi FD. Resistive sensor for acetone vapour. Patent RO 129798 B1. 2017

[2] Fergus JW. Perovskite oxides for semiconductor-based gas sensors. Sensors and Actuators B. 2007;**123**:1169-1179. DOI: 10.1016/j.snb.2006.10.051

[3] Naderer M, Kainz T, Schütz D, Reichmann K. The influence of Ti-nonstoichiometry in $Bi_{0.5}Na_{0.5}TiO_3$. Journal of the European Ceramic Society. 2014;**34**:663-667. DOI: 10.1016/j.jeurceramsoc.2013.10.010

[4] Bukhari SM, Giorgi J. Ni doped $Sm_{0.95}Ce_{0.05}FeO_{3-1}$ perovskite based sensors for hydrogen detection. Sensors and Actuators B. 2013;**181**:153-158. DOI: 10.1016/j.snb.2013.01.073

[5] Bertocci F, Fort A, Vignoli V, Mugnaini M, Berni R. Optimization of perovskite gas sensor performance: Characterization, measurement and experimental design. Sensors. 2017;**17**: 1352-1373. DOI: 10.3390/s17061352

[6] Doroftei C, Popa PD, Iacomi F. Study of the influence of nickel ions substitutes in barium stannates used as humidity resistive sensors. Sensors and Actuators A. 2012;**173**:24-29. DOI: 10.1016/j.sna.2011.10.007

[7] Doroftei C. Formaldehyde sensitive Zn-doped LPFO thin films obtained by rf sputtering. Sensors and Actuators B. 2016;**231**:793-799. DOI: 10.1016/j.snb.2016.03.104

[8] Moseley PT, Norris JOW, Williams DE. Techniques and mechanisms in gas sensing.Bristol, UK: Adam Hilger; 1991. pp. 46-60

[9] Seiyama T, Kato A, Fujisishi K, Nagatoni M. A new detector for gaseous components using semiconductive thin films. Analytical Chemistry. 1962;**34**:1052-1053. DOI: 10.1021/ac60191a001

[10] Carotta MC, Benetti M, Ferrari E, Giberti A, Malagu C, Nagliati M, Vendemiati B, Martinelli G. Basic interpretation of thick film gas sensors for atmospheric application. Sensors and Actuators B. 2007;**126**:672-677. DOI: 10.1016/j.snb.2007.04.016

[11] Frenzer G, Frantzen A, Sanders D, Simion U, Maier WF. Wet chemical synthesis and screening of thick porous films for resistive gas sensing applications. Sensors. 2006;**6**: 1568-1586. DOI: 10.3390/s6111568

[12] Arai H, Ezaki S, Shimizu Y, Shippo O, Seiyama T. Semiconductive humidity sensor of perovskite type oxides. In: Proceedings International Meeting on Chemical Sensors; 19-22 September 1983; Fukuoka. pp. 393-398

[13] Seiyama T, Yamazoe N, Arai H. Ceramic humidity sensors. Sensors and Actuators B. 1983; **4**:85-96. DOI: 10.1016/0250-6874(83)85012-4

[14] Ding J, TJMc A, Cavicchi RE, Semancik S. Surface state trapping model for SnO_2-based microhotplate sensors. Sensors and Actuators B. 2001;**77**:597-601. DOI: 10.1016/S0925-4005(01)00765-1

[15] Chakraborty S, Sen A, Maiti HS. Selective detection of methane and butane by temperature modulation in iron doped tin oxide sensors. Sensors and Actuators B. 2006;**115**:610-613. DOI: 10.1016/j.snb.2005.10.046

[16] Parret F, Menini P, Marlinez A, Soulantica K, Maisonnat A, Chaudret B. Improvement of micromachined SnO_2 gas sensors selectivity by optimised dynamic temperature operating mode. Sensors and Actuators B. 2006;**118**:276-282. DOI: 10.1016/j.snb.2006.04.055

[17] Nakata S, Okunishi H, Nakashima Y. Distinction of gases with a semiconductor sensor under a cyclic temperature modulation with second-harmonic heating. Sensors and Actuators B. 2006;**119**:556-561. DOI: 10.1016/j.snb.2006.01.009

[18] Nakata S, Okunishi H, Nakashima Y. Distinction of gases with a semiconductor sensor depending on the scanning profile of a cyclic temperature. The Analyst. 2006;**131**:148-154. DOI: 10.1039/B509996J

[19] Huang JR, Li GY, Huang ZY, Huang XJ, Liu JH. Temperature modulation and artificial neural network evaluation for improving the CO selectivity of SnO_2 gas sensor. Sensors and Actuators B. 2006;**114**:1059-1063. DOI: 10.1016/j.snb.2005.07.070

[20] Huang JR, Gu CP, Meng FL, Li MQ, Liu JH. Detection of volatile organic compounds (VOCs) by using a single temperature modulated SnO_2 gas sensor and artificial neural network. Smart Materials and Structures. 2007;**16**:701-705

[21] Baschirotto A, Capone S, D'Amico A, Di Natale G, Ferragina V, Ferri G, Francioso L, Grassi M, Guerrini N, Malcovati P, Martinelli E, Siciliano P. A portable integrated widerange gas sensing system with smart A/D front-end. Sensors and Actuators B. 2008; **130**:164-174. DOI: 10.1016/j.snb.2007.07.144

[22] Sysoev VV, Goschnick J, Schneider T, Strelcov E, Kolmakov A. A gradient microarray electronic nose based on percolating SnO_2 nanowire sensing elements. Nano Letters. 2007;**7**:3182-3188. DOI: 10.1021/nl071815+

[23] Rock F, Barsan N, Weimar U. Electronic nose: Current status and future trends. Chemical Reviews. 2008;**108**:705-725. DOI: 10.1021/cr068121q

[24] Wen Z, Tian-mo L. Gas-sensing properties of SnO_2-TiO_2-based sensor for volatile organic compound gas and its sensing mechanism. Physica B: Condensed Matter. 2010;**405**:1345-1348. DOI: 10.1016/j.physb.2009.11.086

[25] Bangale SV, Patil DR, Bamane SR. Nanostructured spinel $ZnFe_2O_4$ for the detection of chlorine gas. Sensors and Transducers Journal. 2011;**134**:107-119

[26] Iftimie N, Rezlescu E, Popa PD, Rezlescu N. Gas sensitivity of nanocrystalline nickel ferrite. Journal of Optoelectronics and Advanced Materials. 2006;**8**:1016-1018

[27] Comini E, Ferroni M, Guidi V, Fagila G, Martinelli G, Sberverglieri G. Nanostructured mixed oxides compounds for gas sensing applications. Sensors and Actuators B. 2002;**84**: 26-32. DOI: 10.1016/S0925-4005(02)00006-0

[28] Reddy CVG, Manorama SV, Rao VJ. Semiconducting gas sensor for chlorine based on inverse spinel nickel ferrite. Sensors and Actuators B. 1999;**55**:90-95. DOI: 10.1016/S0925-4005(99)00112-4

[29] Chen NS, Yang XJ, Liu ES, Huang JL. Reducing gas-sensing properties of ferrite compounds MFe_2O_4 (M = Cu, Zn, Cd and Mg). Sensors and Actuators B. 2000;**66**:178-180. DOI: 10.1016/S0925-4005(00)00368-3

[30] Rezlescu N, Doroftei C, Rezlescu E, Popa PD. Structure and humidity sensitive electrical properties of the Sn^{4+} and/or Mo^{6+} substituted Mg ferrite. Sensors and Actuators B. 2006; **115**:589-595. DOI: 10.1016/j.snb.2005.10.028

[31] Satyanarayana L, Reddy KM, Manorama SV. Synthesis of nanocrystalline $Ni_{1-x}Co_xMn_x Fe_{2-x}O_4$: A material for liquefied petroleum gas sensing. Sensors and Actuators B. 2003;**89**: 62-67. DOI: 10.1016/S0925-4005(02)00429-X

[32] Niu X, Du W, Du W. Preparation and gas sensing properties of ZnM_2O_4 (M = Fe, Co, Cr). Sensors and Actuators B. 2004;**99**:405-409. DOI: 10.1016/j.snb.2003.12.007

[33] Rezlescu N, Doroftei C, Rezlescu E, Popa PD. Lithium ferrite for gas sensing applications. Sensors and Actuators B. 2008;**133**:420-425. DOI: 10.1016/j.snb.2008.02.047

[34] Liu X, Cheng B, Qin H, Song P, Huang S, Zhang R, Hu J, Jiang M. Preparation, electrical and gas sensing properties of perovskite-type $La_{1-x}Mg_xFeO_3$ semiconductor materials. Journal of Physics and Chemistry of Solids. 2007;**68**:511-515. DOI: 10.1016/j.jpcs.2007.01.009

[35] Kapse VD. Preparation of nanocrystalline spinel-type oxide materials for gas sensing applications. Research Journal of Chemical Sciences. 2015;**5**:7-12

[36] Sutkaa A, Mezinskis G, Lusis A, Stingaciuc M. Gas sensing properties of Zn-doped p-type nickel ferrite. Sensors and Actuators B. 2012;**171–172**:354-360. DOI: 10.1016/j.snb.2012.04.059

[37] Wang N, Hu CG, Xia CH, Feng B, Zhang WZ, Xi Y, Xiong YF. Ultrasensitive gas sensitivity property of $BaMnO_3$ nanorods. Applied Physics Letters. 2007;**90**:163111.1-163111.3. DOI: 10.1063/1.2722692

[38] Hara T, Ishiguro T, Wakiya N, Shinozaki K. Oxigen sensing properties of $SrTiO_3$ thin films. Japanese Journal of Applied Physics. 2008;**47**:7486-7489. DOI: 10.1143/JJAP.47.7486

[39] Chaudhari GN, Padole PR, Jagatap SV, Pawar MJ. CO_2 sensing characteristics of $Sm_{1-x}Ba_xCoO_3$ (x = 0; 0.1; 0.15; 0.2) nanostructured thick film. International Journal on Smart Sensing and Intelligent Systems. 2008;**1**:613-622

[40] Rezlescu N, Rezlescu E, Popa PD, Doroftei C, Ignat M. Comparative study between catalyst properties of simple spinel ferrite powders prepared by self-combustion route. Romanian Reports in Physics. 2013;**65**:1348-1356

[41] Doroftei C, Leontie L, Popa A. The study on nanogranular system manganites La-Pb--Ca-Mn-O which exhibits a large magnetoresistance near room temperature. Journal of Materials Science-Materials in Electronics. 2017;**28**:12891-12899. DOI: 10.1007/s10854-017-7119-8

[42] Doroftei C, Popa PD, Rezlescu E, Rezlescu N. Structural and catalytic characterization of nanostructured iron manganite. Composites: Part B. 2014;**67**:179-182. DOI: 10.1016/j.compositesb.2014.07.005

[43] Rezlescu N, Rezlescu E, Popa PD, Doroftei C, Ignat M. Some nanograined ferrites and perovskites for catalytic combustion of acetone at low temperature. Ceramics International. 2015;**41**:4430-4437. DOI: 10.1016/j.ceramint.2014.11.134

[44] Rezlescu N, Rezlescu E, Popa PD, Doroftei C, Ignat M. Scandium substituted nickel-cobalt ferrites nanoparticles for catalyst applications. Applied Catalysis B. 2014;**158**:70-75. DOI: 10.1016/j.apcatb.2014.03.052

[45] Rezlescu N, Rezlescu E, Popa PD, Doroftei C, Ignat M. Nanostructured $GdAlO_3$ perovskite, a new possible catalyst for combustion of volatile organic compounds. Journal of Materials Science. 2013;**48**:4297-4304. DOI: 10.1007/s10853-013-7243-7

[46] Doroftei C, Popa PD, Rezlescu E, Rezlescu N. Nanocrystalline $SrMnO_3$ powder as catalyst for hydrocarbon combustion. Journal of Alloys and Compounds. 2014;**584**:195-198. DOI: 10.1016/j.jallcom.2013.09.054

[47] Doroftei C, Popa PD, Iacomi F. Synthesis of nanocrystalline La-Pb-Fe-O perovskite and methanol sensing. Sensors and Actuators B. 2012;**161**:977-981. DOI: 10.1016/j.snb.2011.11.078

[48] Leontie L, Doroftei C. Nanostructured spinel ferrites for catalytic combustion of gasoline vapors. Catalysis Letters. 2017;**147**:2542-2548. DOI: 10.1007/s10562-017-2164-8

[49] Doroftei C, Leontie L. Synthesis and characterization of some nanostructured composite oxides for low temperature catalytic combustion of dilute propane. RCS Advances. 2017;**7**: 27863-27871. DOI: 10.1039/c7ra03916f

[50] Rezlescu N, Doroftei C, Rezlescu E, Popa PD. The influence of Sn^{4+} and/or Mo^{6+} ions on the structure, electrical and gas sensing properties of Mg-ferrite. Physica Status Solidi A. 2006;**203**:306-316. DOI: 10.1002/pssa.200521043

[51] Doroftei C, Popa PD, Iacomi F, Leontie L. The influence of Zn^{2+} ions on the microstructure, electrical and gas sensing properties of $La_{0.8}Pb_{0.2}FeO_3$ perovskite. Sensors and Actuators B. 2014;**191**:239-245. DOI: 10.1016/j.snb.2013.09.113

[52] D'Amico A, Di Natale C. A contribution on some basic definitions of sensors properties. IEEE Sensors Journal. 2001;**1**:183-190. DOI: 10.1109/JSEN.2001.954831

[53] Doroftei C, Popa PD, Iacomi F. Selectivity between methanol and ethanol gas of La-Pb-Fe-O perovskite synthesized by novel method. Sensors and Actuators A. 2013;**190**:176-180. DOI: 10.1016/j.sna.2012.11.018

[54] Zhang L, Qin HW, Song P, Hu JF, Jiang MH. Electric properties and acetone-sensing characteristics of $La_{1-x}Pb_xFeO_3$ perovskite system. Materials Chemistry and Physics. 2006;**98**:358-362. DOI: 10.1016/j.matchemphys.2005.09.041

[55] Song P, Qin HV, Zhang L, An K, Lin ZI, Hu JF, Jiang MH. The structure, electrical and ethanol-sensing properties of $La_{1-x}Pb_xFeO_3$ perovskite ceramicswith $x \leq 0.3$. Sensors and Actuators B. 2005;**104**:312-316. DOI: 10.1016/j.snb.2004.05.023

[56] Singh MP, Singh H, Singh O, Kohli N, Singh RC. Preparation and characterization of nanocrystalline WO_3 powder based highly sensitive acetone sensor. Indian Journal of Physics. 2012;**86**:357-361. DOI: 10.1007/s12648-012-0062-x

[57] Martins R, Fortunato E, Nunes P, Fereira I, Marques A. Zinc oxide as an ozone sensor. Journal of Applied Physics. 2004;**96**:1398-1408. DOI: 10.1063/1.1765864

IntechOpen